Check for updates

How to cite: *Angew. Chem. Int. Ed.* **2021**, *60*, 25695–25700
International Edition: doi.org/10.1002/anie.202109840
German Edition: doi.org/10.1002/ange.202109840

Helicenes

A Modular Cascade Synthetic Strategy Toward Structurally Constrained Boron-Doped Polycyclic Aromatic Hydrocarbons

Jin-Jiang Zhang, Lin Yang, Fupin Liu, Yubin Fu, Junzhi Liu, Alexey A. Popov, Ji Ma, and Xinliang Feng**

Abstract: *A novel synthetic strategy was developed for the construction of difficult-to-access structurally constrained boron-doped polycyclic aromatic hydrocarbons (sc-B-PAHs) via a cascade reaction from the readily available ortho-aryl-substituted diarylalkynes. This domino process involves borylative cyclization, 1,4-boron migration and successive two-fold electrophilic borylation. Two types of sc-B-PAHs bearing B-doped [4]helicene (**1a-1i**) or BN-doped [4]helicene (**1n-1t**) and double [4]helicene (**1u-1v**) are constructed by this cascade reaction. Remarkably, this synthetic strategy is characterized by modest yields (20–50%) and broad substrate scope (18 examples) with versatile functional group tolerance. The resultant sc-B-PAHs show good stability under ambient conditions and are thoroughly investigated by X-ray crystallography, UV/Vis absorption and fluorescence spectroscopy, and cyclic voltammetry. Interestingly enough, BN-doped [4]helicene **1o** forms a unique alternating π-stacked dimer of enantiomers within a helical columnar superstructure, while BN-doped double [4]helicene **1u** establishes an unprecedented π-stacked trimeric sandwich structure with a rare 2D lamellar π-stacking. The synthetic approach reported herein represents a powerful tool for the rapid generation of novel sc-B-PAHs, which are highly attractive for the elucidation of the structure-property relationship and for potential optoelectronic applications.*

The incorporation of main group elements such as B, N, or S into polycyclic aromatic hydrocarbons (PAHs) has proven to be a powerful strategy to modulate the physicochemical properties of the parent π-conjugated systems, such as chemical reactivity, electronic energy gap, redox behavior and supramolecular organization in the solid state.[1] In particular, boron incorporation has attracted great interest in the last decade due to its excellent ability to modify the optoelectronic properties of PAHs, e.g., to provide the resulting systems with intense luminescence, high electron deficiency, strong Lewis acidity, and bestowing the resultant compounds with unique supramolecular behavior.[2] In the design of boron-doped PAHs (B-PAHs), three strategies have been explored so far to address their stability problems, including electronic effect,[3] steric effect,[4] and chelating effect[5] (Figure 1a). However, the benchtop-stable B-PAHs obtained by applying electronic/kinetic stabilization approach generally sacrificed the Lewis acid character of the boron center and diminished its intermolecular interaction in the solid state. In contrast, structurally constrained B-PAHs (sc-B-PAHs) stabilized by the chelating effect are expected to enable tight intermolecular packing and enhance the intermolecular interaction in the solid state, therefore improving the charge carrier transport properties.[2b,d] Moreover, sc-B-PAHs are capable of forming Lewis acid-base complexes which can undergo photodissociation in the excited state, giving a dual fluorescence emission.[5b,g] Nevertheless, the related studies on sc-B-PAHs are relatively rare due to the limited synthetic approaches.

The pioneering work toward sc-B-PAHs was disclosed by Yamaguchi's group in 2012; they synthesized the π-extended planarized triarylborane compound **I** (Figure 1b) by combining a radical initiated dehalogenative cyclization with an intramolecular oxidative cyclization.[5a] Later on, Wagner et al. demonstrated that the Yamamoto coupling reaction serves as a feasible strategy for the preparation of sc-B-PAHs, e.g., in the synthesis of B-doped [4]helicene molecule **II**.[5d] Shortly thereafter, Hatakeyama et al. obtained the same compound via a one-pot synthetic method involving lithium/boron exchange and intramolecular electrophilic borylation.[5e] In 2016, Ingleson and co-workers disclosed a one-pot inter/intramolecular C–H borylation towards sc-B-PAHs **III** from the electron-rich indole structure.[6] Besides of solely boron containing PAHs, these synthetic strategies, including

[*] J.-J. Zhang, L. Yang, Dr. Y. Fu, Dr. J. Ma, Prof. Dr. X. Feng
Center for Advancing Electronics Dresden (cfaed) & Faculty of Chemistry and Food Chemistry, Technische Universität Dresden
Mommsenstrasse 4, 01062 Dresden (Germany)
E-mail: ji.ma@tu-dresden.de
xinliang.feng@tu-dresden.de
Dr. F. Liu, Dr. A. A. Popov
Center of Spectroelectrochemistry, Leibniz Institute for Solid State and Materials Research (IFW) Dresden
Helmholtzstrasse 20, 01069 Dresden (Germany)
Dr. J. Liu
Department of Chemistry and State Key Laboratory of Synthetic Chemistry, The University of Hong Kong
Pokfulam Road, Hong Kong (China)
Prof. Dr. X. Feng
Max Planck Institute of Microstructure Physics
Weinberg 2, 06120 Halle (Germany)
Supporting information and the ORCID identification number(s) for the author(s) of this article can be found under: https://doi.org/10.1002/anie.202109840.

© 2021 The Authors. Angewandte Chemie International Edition published by Wiley-VCH GmbH. This is an open access article under the terms of the Creative Commons Attribution Non-Commercial NoDerivs License, which permits use and distribution in any medium, provided the original work is properly cited, the use is non-commercial and no modifications or adaptations are made.

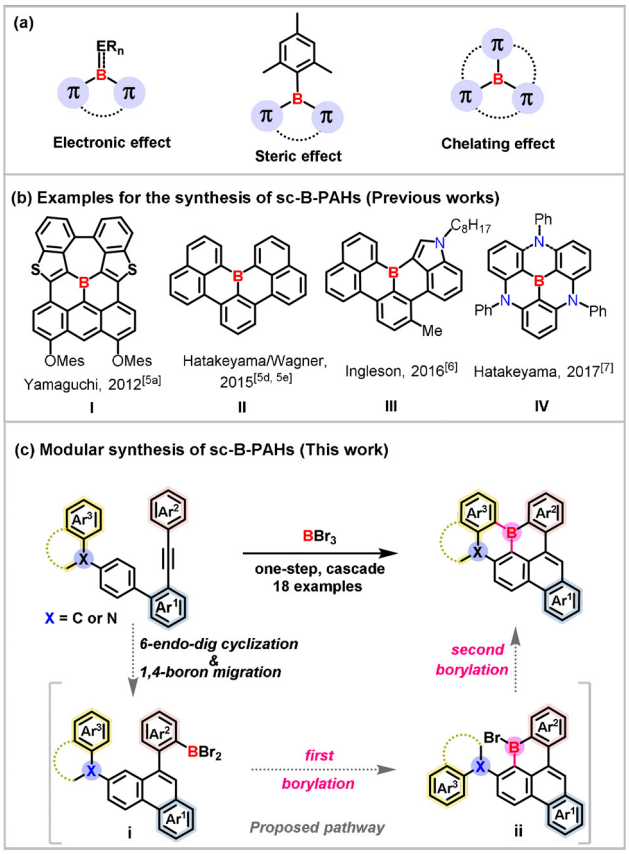

Figure 1. a) Three strategies for making bench-stable B-PAHs; b) Representative examples regarding sc-B-PAHs; c) One-step cascade synthesis of sc-B-PAHs in this work.

the lithium/boron exchange method and direct borylative reaction, were also utilized for synthesizing N-bridged B-doped triangulene **IV** by Hatakeyama's group.[7] Despite considerable progress, the aforementioned cases face drawbacks like low functional group tolerance and limited applicability. To date, there is still a lack of facile and broadly applicable synthetic route towards the sc-B-PAHs.

Herein, we demonstrate a modular and straightforward synthetic route via a one-step cascade reaction from the easily accessed alkyne precursors to construct a series of novel mono/dual sc-B-PAHs (**1a**-**1v**) bearing B-doped [4]helicene subunits or BN-doped [4]helicene motifs.[8] (Figure 1c). Our synthetic strategy involves the sequential 6-endo-dig cyclization,[9] 1,4-boron migration[4f] and successive two-fold electrophilic borylation, leading to the formation of four bonds (one C–C, three C–B bonds) and three six-membered rings in one step. Importantly, this approach also features a broad scope of substrates (18 examples) since the three different aryl parts of substrate (Ar^1, Ar^2 and Ar^3) could be replaced by various motifs and substituents. Single-crystal analysis of **1e**, **1o** and **1u** unveils the twisted scaffold with a dihedral angle from 19.95° (**1o**) to 23.49° (**1e**) in the cove region of [4]helicene. Notably, in the solid-stack packing pattern, **1o** forms a unique alternating π-stacked dimer of enantiomers (M and P) which self-organizes into a π-stacking helical columnar superstructure, while **1u** establishes an unprecedented π-stacked trimeric structure and adopts a unique 2D lamellar π-stacking. Moreover, the optical energy gaps of sc-B-PAHs **1a**-**1v** range from 2.36 eV (**1u**) to 2.73 eV (**1n**) and most of the obtained sc-B-PAHs display strong fluorescence with the photoluminescence (PL) quantum yields (Φ_{PL}) ranging from 24% to 85% in dichloromethane solution.

To achieve the synthesis of sc-B-PAHs via the domino process in this work, multiple feasible borylation sites need to be introduced into the precursor (Figure 1c). In consideration of this, 1-(2′-(phenylethynyl)-[1,1′-biphenyl]-4-yl)naphthalene (**2a**) was chosen as a model substrate at the outset, we assumed that compound **2a** would undergo a sequential 6-endo-dig cyclization and 1,4-boron migration process to furnish the crucial intermediate **i**; then **i** will undergo the first-time electrophilic borylation to afford the six-membered boracycle **ii**; finally the naphthalene ring could provide another reaction site for the second electrophilic borylation to achieve the targeted sc-B-PAHs (Figure 1c). To prove this hypothesis, boron tribromide (BBr_3) was added into the 1,2,4-trichlorobenzene (TCB) solution of **2a** and 2,4,6-tri-*tert*-butylpyridine (TBP), then the mixture was heated at 200 °C for 12 hours. Remarkably, the desired sc-B-PAH **1a** was obtained in 28% yield. Inspired by this preliminary result, a variety of analogues (**2b**–**2m**) of **2a** were performed under standard conditions to investigate the substrate scope (Table 1). Most of the substrates were efficiently incorporated into this cascade reaction pathway to yield the corresponding sc-B-PAHs **1b**–**1i** in a moderate yield from 18% (**1b**) to 40% (**1g**). It is noteworthy that halogen (Br or Cl) and cyano (CN) groups can be tolerated under the current conditions (**1e**, **1f**, and **1i**), offering the possibility for the post-functionalization of this class of compounds. Unfortunately, no desired compound was detected for **2j**, **2k**, **2l** and **2m** bearing the dimethylamine (in Ar^1), pyridine (Ar^1 and Ar^2) or trifluoromethyl substituent (Ar^2), possibly because they can interact with BBr_3 or activated arylborane intermediates and therefore quench the reaction.

Instead of the naphthalene ring in the Ar^3 part which can provide second borylation sites in the domino reaction, we hypothesized that the N,N-diphenyl group in Ar^3 could not only play the same role, but also increase the electron density of the borylation sites and reduce the steric hindrance during the reaction, which in principle could facilitate the reaction.[7d]

Therefore, we further explored the applicability of this strategy by replacing the naphthalene ring in Ar^3 with N,N-diphenyl group for the synthesis of B/N co-doped PAHs (Table 2). Remarkably, when N,N-diphenyl-2′-(phenylethynyl)-[1,1′-biphenyl]-4-amine (**2n**) was treated under the standard conditions, sc-B-PAH bearing BN-doped [4]helicene (**1n**) was obtained in a decent yield (58%). By replacing the benzene ring in Ar^1 part with more electron-rich naphthalene motif (**2o**) or carbazole substituted phenyl ring (**2p**), the yield of desired compounds could be further improved (**1o**: 73%; **1p**: 76%). Satisfactorily, this synthetic strategy could be scaled up to a gram scale (**1o**, 1.5 g). Nevertheless, the reaction was dramatically inhibited when the carbazole group was installed in **2r** instead of *N*,*N*-diphenyl group, furnishing **1r** in 8% yield. The low yield of **1r** could be ascribed to the planar and rigid structure of the carbazole moiety in **2r**, which

 © 2021 The Authors. Angewandte Chemie International Edition published by Wiley-VCH GmbH

Table 1: Scope of one-step cascade synthesis of [4]helicene-containing sc-B-PAHs **1a-1i**.[a]

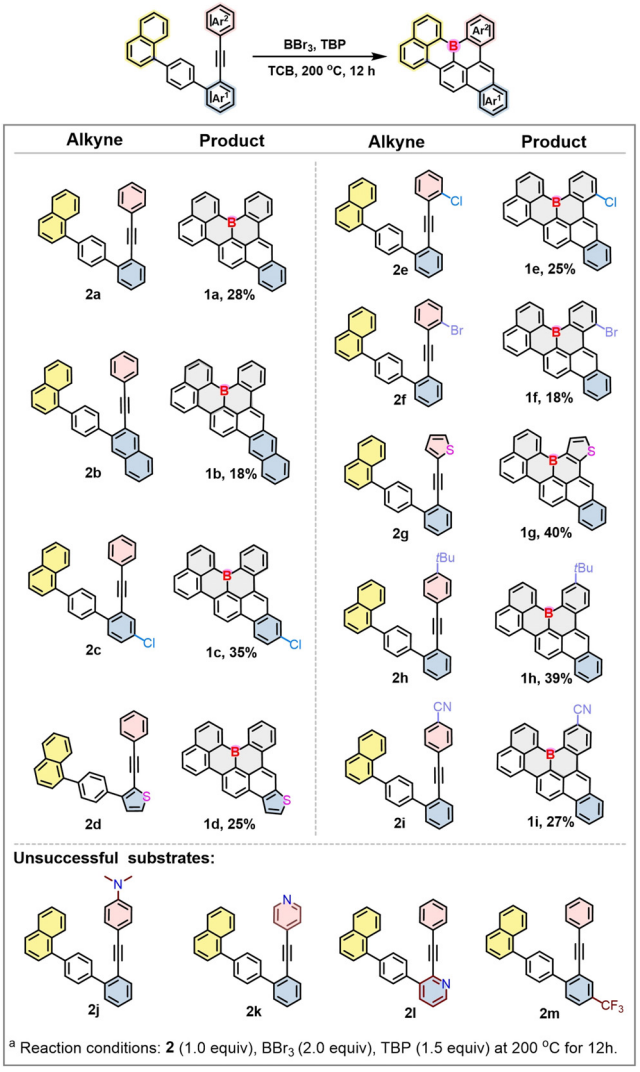

[a] Reaction conditions: **2** (1.0 equiv), BBr_3 (2.0 equiv), TBP (1.5 equiv) at 200 °C for 12h.

Table 2: Scope of one-step cascade synthesis of BN-doped [4]helicene containing sc-B-PAHs **1n-1v**.[a]

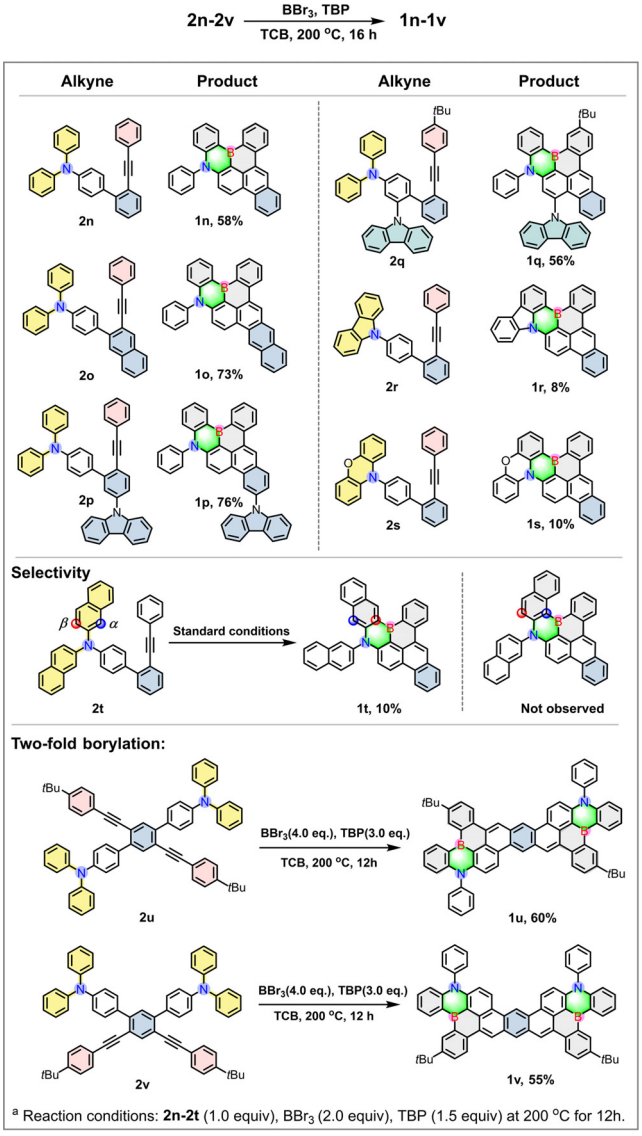

[a] Reaction conditions: **2n-2t** (1.0 equiv), BBr_3 (2.0 equiv), TBP (1.5 equiv) at 200 °C for 12h.

would result in the borylation reaction sites being further away from the six-membered boracycle intermediate **ii**. Therefore, the second time electrophilic borylation becomes more difficult than the flexible N,N-diphenyl subunit in **2n**.[10] We further investigated the selectivity of the second borylation reaction using *N,N*-dinaphthalene substituted precursor **2t**. It was shown that the second time electrophilic borylation occurred at the less active "β-position" on the naphthalene ring, giving **1t** in 10% yield, without the detection of "α-position" borylated product. This result should be ascribed to the less steric crowding of "β-position" compared with "α-position". In order to further demonstrate the utility of this strategy, we proceeded to target the extended sc-B-PAHs containing two boron centers. To our delight, BN-doped double [4]helicene **1u** and **1v** were successfully achieved from **2u** and **2v** with a yield of 60% and 55%, respectively. Therefore, our results clearly demonstrate the vast potential of this synthetic strategy toward the expanded and helical PAHs containing with multiple B/N atoms.

The chemical structures of the representative heterohelicenes **1e**, **1o** and **1u** were unequivocally revealed by the X-ray crystallographic analysis. It also enables the investigation of the impact of B/N doping on their solid-state packing behavior (Figure 2). All of these three compounds display a nonplanar geometry due to the existence of [4]helicene substructure, with a torsional angle of 23.49° (**1e**), 19.95° (**1o**) and 22.79° (**1u**), respectively. In addition, all of them show a twist conformation at the bay region and the dihedral angle are 26.75° (**1e**), 7.22° (**1o**) and 16.87° (**1u**), respectively. The three C–B bond lengths are in the range of 1.513–1.515 Å (Table S2), indicating single C–B bond character. Notably, the three C–B bonds length in **1e**, **1o** and **1u** all show the following trend: C_2-B_1 > C_1-B_1 > C_3-B_1, which could result from a successive increase in the degree of π-conjugation between boron center and adjacent arene units (C_2 unit < C_1 unit < C_3 unit).[11] In the solid state, the unit cell of **1e** contains two enantiomers (M and P) and they are further packed into

 © 2021 The Authors. Angewandte Chemie International Edition published by Wiley-VCH GmbH

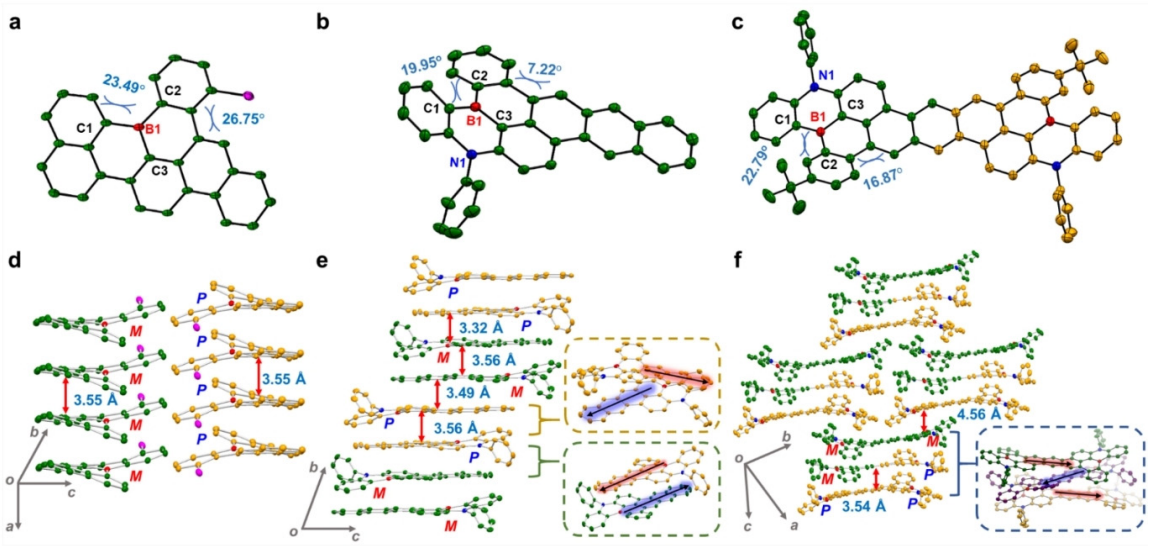

Figure 2. X-ray crystallographic molecular structures of **1e** (a), **1o** (b), **1u** (c), (C: green/orange, B: red, Cl: purple, N: blue. H atoms are omitted for clarity) and packing arrangements of **1e** (d), **1o** (e), **1u** (f).[13]

an ordered columnar arrangement with a π-stacking distance of 3.55 Å, respectively (Figure 2d). In contrast to **1e**, two enantiomers (M and P) of **1o** form the π-stacked dimer which are arranged in a unique alternating helical columnar superstructure, in which the neighboring hetero-enantiomers adopt an antiparallel stacking and the homo-enantiomers are rotated by 120° against each other to avoid steric hindrance. This unique solid-state packing has been rarely observed.[12] The enantiomers form strong π···π interactions along the *b*-axis with distances of 3.32–3.56 Å (Figure 2e). Most interestingly, for double [4]helicene **1u**, three conformers (M/M, M/P and P/P) are found in a unit cell, thus forming an unprecedented trimeric superstructure in which the conformer (M/P) is sandwiched and helically arranged between the enantiomers (M/M and P/P) with a distance of 3.54 Å. The unit cell of **1u** clearly reveals a 2D "bricklayer" arrangement, in which the distance of two trimeric packs is 4.56 Å (Figure 2f). This unprecedented stacking pattern of **1u** suggests the unique role of B/N doping on modulating the supramolecular behavior.

The UV/Vis absorption and fluorescence spectra of **1a**-**1v** were recorded in anhydrous dichloromethane (CH_2Cl_2) solution. For B-doped [4]helicene **1a**-**1i**, the longest-wavelength absorption peaks range from 453 (**1c**) to 490 nm (**1b**) (Figure 3a). The maximum absorption peaks are located in the visible region from 440 (**1n**) to 510 nm (**1u**) for BN-doped [4]helicenes **1n**-**1v** (Figure 3b). Therefore, the measured optical energy gaps for **1a**-**1v** range from 2.36 eV (**1u**) to 2.73 eV (**1n**). Interestingly, N-bridged compounds **1n** and **1o** exhibit a blue-shift of 15 nm compared to its similar backbone analogues **1a** and **1b**, possibly because of the lower π-conjugation of N,N-diphenyl moiety compared with naphthalene ring. Fluorescence spectroscopy reveals that the emission band maxima for **1a**-**1v** falls in the range between 449 (**1i**) and 545 nm (**1b**) (Figure 3c, d). Upon excitation, **1a**-**1v** exhibit strong fluorescence with photoluminescence (PL) quantum yields (Φ_{PL}) up to 85% (**1i**) (Table S1).

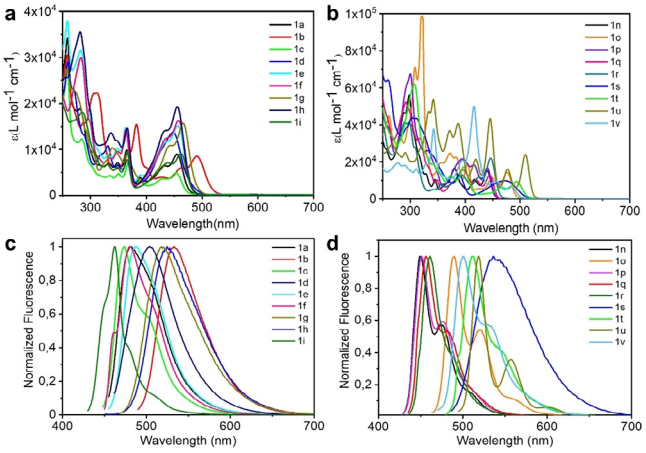

Figure 3. UV/Vis absorption (a, b) and fluorescence (c, d) spectra of **1a**-**1v** (10^{-6} M in CH_2Cl_2).

To gain insight into the electronic structure of this series of sc-B-PAHs, DFT calculation was performed at the B3LYP/6-31G(d) level (Figures S72-S89). The calculated results for the representative compounds **1a**, **1n**, **1p** and **1u** are summarized in Figure 4a. The BN-doped [4]helicene **1n** displays 0.25 eV higher energy level of HOMO than that of B-doped [4]helicene **1a**, which can be attributed to the larger contributions of nitrogen to its HOMO. Besides, the LUMO energy of **1a** is found to be around 0.6 eV lower than that of **1n**, which is attributed to the larger contribution to the LUMO from the naphthalene ring. Notably, the carbazole unit in **1p** enables to establish a donor-acceptor structure with the embedded boron center, resulting in the orbital separation. In addition, the anisotropy of the induced current density (ACID) and nucleus independent chemical shifts (NICS) calculations indicate that the benzene rings and the BNC_4 ring display an aromatic feature while the boron-embedded six-membered rings exhibit non-aromatic character (Figure 4b).

 © 2021 The Authors. Angewandte Chemie International Edition published by Wiley-VCH GmbH

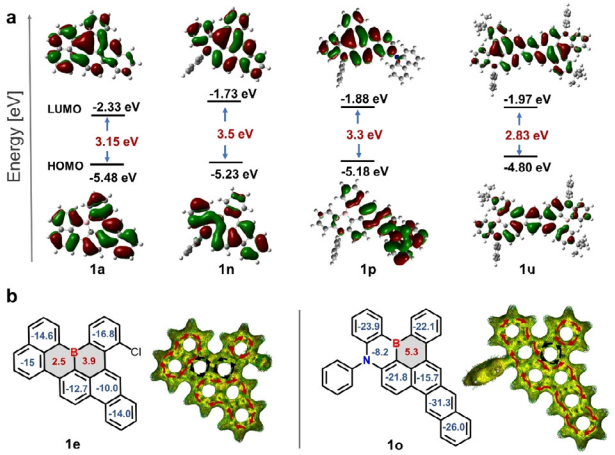

Figure 4. a) Calculated frontier molecular orbital profiles and energy diagram of represented compounds. b) NICS(0)zz values and ACID plots (red circle: aromatic ring; black circle: anti-aromatic ring) of represented compounds **1e** and **1o**.

In conclusion, we herein reported an efficient synthetic strategy to obtain a new family of sc-B-PAHs via a one-step cascade reaction, involving 6-endo-dig cyclization, 1,4-boron migration and successive two-fold electrophilic borylation. This domino process features simplicity and a broad substrate scope. Not only sc-B-PAHs with B-doped [4]helicene structure but also specific BN-doped [4]helicene/double-[4]helicene can be constructed by this approach. Noteworthily, the resultant BN-doped [4]helicene demonstrate distinct supramolecular behavior in the solid state, for example, mono [4]helicene **1o** forms a unique π-stacked dimer and adopts helical columnar stacking, while double [4]helicene **1u** establishes an unprecedented π-stacked trimeric structure with a 2D lamellar π-stacking. The presented strategy thus provides a new pathway for the development of novel sc-B-PAHs and expanded B-doped graphene nanostructures. Further studies on the application of this boron-embedded π-system are currently ongoing in our laboratory.

Acknowledgements

This research was financially supported by the EU Graphene Flagship (Graphene Core 3, 881603), ERC Consolidator Grant (T2DCP, 819698), the Center for Advancing Electronics Dresden (cfaed) and DFG-NSFC Joint Sino-German Research Project (EnhanceNano, No. 391979941), as well as the DFG-SNSF Joint Switzerland-German Research Project (EnhanTopo, No. 429265950). The authors acknowledge the use of computational facilities at the Center for information services and high performance computing (ZIH) at TU Dresden. Diffraction data have been collected on BL14.2 at the BESSY II electron storage ring operated by the Helmholtz-Zentrum Berlin, we thank Dr. Manfred Weiss and his team for assistance during the experiment. Open Access funding enabled and organized by Projekt DEAL.

Conflict of Interest

The authors declare no conflict of interest.

Keywords: boron doping · helicenes · polycyclic aromatic hydrocarbons · structure constraint · supramolecular behavior

[1] a) X. Wang, G. Sun, P. Routh, D.-H. Kim, W. Huang, P. Chen, *Chem. Soc. Rev.* **2014**, *43*, 7067–7098; b) A. Mateo-Alonso, *Chem. Soc. Rev.* **2014**, *43*, 6311–6324; c) M. Stepien, E. Gonka, M. Zyla, N. Sprutta, *Chem. Rev.* **2017**, *117*, 3479–3716; d) S. M. Parke, M. P. Boone, E. Rivard, *Chem. Commun.* **2016**, *52*, 9485–9505; e) D. Wu, W. Pisula, M. C. Haberecht, X. F. Feng, K. Müllen, *Org. Lett.* **2009**, *11*, 5686–5689; f) D. Wu, W. Pisula, V. Enkelmann, X. F. Feng, K. Müllen, *J. Am. Chem. Soc.* **2009**, *131*, 9620–9621; g) W. Pisula, X. Feng, K. Müllen, *Adv. Mater.* **2010**, *22*, 3634–3649.

[2] a) E. von Grotthuss, A. John, T. Kaese, M. Wagner, *Asian J. Org. Chem.* **2018**, *7*, 37–53; b) M. Hirai, N. Tanaka, M. Sakai, S. Yamaguchi, *Chem. Rev.* **2019**, *119*, 8291–8331; c) Z. Huang, S. Wang, R. D. Dewhurst, N. V. Ignat'ev, M. Finze, H. Braunschweig, *Angew. Chem. Int. Ed.* **2020**, *59*, 8800–8816; *Angew. Chem.* **2020**, *132*, 8882–8900; d) X. Y. Wang, F. D. Zhuang, R. B. Wang, X. C. Wang, X. Y. Cao, J. Y. Wang, J. Pei, *J. Am. Chem. Soc.* **2014**, *136*, 3764–3767.

[3] a) P. G. Campbell, A. J. Marwitz, S. Y. Liu, *Angew. Chem. Int. Ed.* **2012**, *51*, 6074–6092; *Angew. Chem.* **2012**, *124*, 6178–6197; b) F.-D. Zhuang, Z.-H. Sun, Z.-F. Yao, Q.-R. Chen, Z. Huang, J.-H. Yang, J.-Y. Wang, J. Pei, *Angew. Chem. Int. Ed.* **2019**, *58*, 10708–10712; *Angew. Chem.* **2019**, *131*, 10818–10822; c) T. Hatakeyama, S. Hashimoto, S. Seki, M. Nakamura, *J. Am. Chem. Soc.* **2011**, *133*, 18614–18617; d) X. Y. Wang, A. Narita, W. Zhang, X. Feng, K. Müllen, *J. Am. Chem. Soc.* **2016**, *138*, 9021–9024; e) X. Y. Wang, A. Narita, X. Feng, K. Müllen, *J. Am. Chem. Soc.* **2015**, *137*, 7668–7671; f) J. Huang, Y. Li, *Front. Chem.* **2018**, *6*, 341.

[4] a) V. M. Hertz, M. Bolte, H. W. Lerner, M. Wagner, *Angew. Chem. Int. Ed.* **2015**, *54*, 8800–8804; *Angew. Chem.* **2015**, *127*, 8924–8928; b) D. L. Crossley, R. J. Kahan, S. Endres, A. J. Warner, R. A. Smith, J. Cid, J. J. Dunsford, J. E. Jones, I. Vitorica-Yrezabal, M. J. Ingleson, *Chem. Sci.* **2017**, *8*, 7969–7977; c) J. M. Farrell, C. Mutzel, D. Bialas, M. Rudolf, K. Menekse, A. M. Krause, M. Stolte, F. Wurthner, *J. Am. Chem. Soc.* **2019**, *141*, 9096–9104; d) A. John, M. Bolte, H. W. Lerner, M. Wagner, *Angew. Chem. Int. Ed.* **2017**, *56*, 5588–5592; *Angew. Chem.* **2017**, *129*, 5680–5684; e) Y. Xia, M. Zhang, S. Ren, J. Song, J. Ye, M. G. Humphrey, C. Zheng, K. Wang, X. Zhang, *Org. Lett.* **2020**, *22*, 7942–7946; f) J. J. Zhang, M. C. Tang, Y. Fu, K. H. Low, J. Ma, L. Yang, J. J. Weigand, J. Liu, V. W. Yam, X. Feng, *Angew. Chem. Int. Ed.* **2021**, *60*, 2833–2838; *Angew. Chem.* **2021**, *133*, 2869–2874.

[5] a) S. Saito, K. Matsuo, S. Yamaguchi, *J. Am. Chem. Soc.* **2012**, *134*, 9130–9133; b) K. Matsuo, S. Saito, S. Yamaguchi, *J. Am. Chem. Soc.* **2014**, *136*, 12580–12583; c) J. Radtke, K. Schickedanz, M. Bamberg, L. Menduti, D. Schollmeyer, M. Bolte, H.-W. Lerner, M. Wagner, *Chem. Sci.* **2019**, *10*, 9017–9027; d) K. Schickedanz, T. Trageser, M. Bolte, H. W. Lerner, M. Wagner, *Chem. Commun.* **2015**, *51*, 15808–15810; e) F. Miyamoto, S. Nakatsuka, K. Yamada, K. Nakayama, T. Hatakeyama, *Org. Lett.* **2015**, *17*, 6158–6161; f) K. Fujimoto, J. Oh, H. Yorimitsu, D. Kim, A. Osuka, *Angew. Chem. Int. Ed.* **2016**, *55*, 3196–3199; *Angew. Chem.* **2016**, *128*, 3248–3251; g) N. Ando, T. Yamada, H. Narita, N. N. Oehlmann, M. Wagner, S. Yamaguchi, *J. Am. Chem. Soc.* **2021**, *143*, 9944–9951.

 © 2021 The Authors. Angewandte Chemie International Edition published by Wiley-VCH GmbH

[6] A. Escande, D. L. Crossley, J. Cid, I. A. Cade, I. Vitorica-Yrezabal, M. J. Ingleson, *Dalton Trans.* **2016**, *45*, 17160 – 17167.
[7] a) S. Nakatsuka, H. Gotoh, K. Kinoshita, N. Yasuda, T. Hatakeyama, *Angew. Chem. Int. Ed.* **2017**, *56*, 5087 – 5090; *Angew. Chem.* **2017**, *129*, 5169 – 5172; b) H. Hirai, K. Nakajima, S. Nakatsuka, K. Shiren, J. Ni, S. Nomura, T. Ikuta, T. Hatakeyama, *Angew. Chem. Int. Ed.* **2015**, *54*, 13581 – 13585; *Angew. Chem.* **2015**, *127*, 13785 – 13789; c) Y. Kondo, K. Yoshiura, S. Kitera, H. Nishi, S. Oda, H. Gotoh, Y. Sasada, M. Yanai, T. Hatakeyama, *Nat. Photonics* **2019**, *13*, 678 – 682; d) K. Matsui, S. Oda, K. Yoshiura, K. Nakajima, N. Yasuda, T. Hatakeyama, *J. Am. Chem. Soc.* **2018**, *140*, 1195 – 1198.
[8] a) T. Agou, J. Kobayashi, T. Kawashima, *Org. Lett.* **2006**, *8*, 2241 – 2244; b) T. Agou, T. Kojima, J. Kobayashi, T. Kawashima, *Org. Lett.* **2009**, *11*, 3534 – 3537.
[9] A. J. Warner, J. R. Lawson, V. Fasano, M. J. Ingleson, *Angew. Chem. Int. Ed.* **2015**, *54*, 11245 – 11249; *Angew. Chem.* **2015**, *127*, 11397 – 11401.
[10] a) W. Yang, R. Bam, V. J. Catalano, W. A. Chalifoux, *Angew. Chem. Int. Ed.* **2018**, *57*, 14773 – 14777; *Angew. Chem.* **2018**, *130*, 14989 – 14993; b) P. M. Donovan, L. T. Scott, *J. Am. Chem. Soc.* **2004**, *126*, 3108 – 3112.
[11] V. M. Hertz, N. Ando, M. Hirai, M. Bolte, H.-W. Lerner, S. Yamaguchi, M. Wagner, *Organometallics* **2017**, *36*, 2512 – 2519.
[12] C. Zeng, C. Xiao, X. Feng, L. Zhang, W. Jiang, Z. Wang, *Angew. Chem. Int. Ed.* **2018**, *57*, 10933 – 10937; *Angew. Chem.* **2018**, *130*, 11099 – 11103.
[13] Deposition Number(s) 2087046 (for 1e), 2087048 (for 1o), 2087049 (for 1u) contain(s) the supplementary crystallographic data for this paper. These data are provided free of charge by the joint Cambridge Crystallographic Data Centre and Fachinformationszentrum Karlsruhe Access Structures service www.ccdc.cam.ac.uk/structures.

Manuscript received: July 22, 2021
Revised manuscript received: October 7, 2021
Accepted manuscript online: October 8, 2021
Version of record online: November 5, 2021

 © 2021 The Authors. Angewandte Chemie International Edition published by Wiley-VCH GmbH